Biosensors and Bioelectronics 82 (2016) 127–131

Contents lists available at ScienceDirect

Biosensors and Bioelectronics

journal homepage: www.elsevier.com/locate/bios

Detection system based on magnetoelastic sensor for classical swine fever virus

Xing Guo, Shuang Gao, Shengbo Sang *, Aoqun Jian, Qianqian Duan, Jianlong Ji, Wendong Zhang

MicroNano System Research Center, Key Lab of Advanced Transducers and Intelligent Control System of the Ministry of Education & College of Information Engineering, Taiyuan University of Technology, Taiyuan 030024, China

ARTICLE INFO

Article history:
Received 4 January 2016
Received in revised form
23 March 2016
Accepted 25 March 2016
Available online 26 March 2016

Keywords:
ME biosensor
CSFV
Detection system
Test paper
Measurement circuit

ABSTRACT

In this paper, a magnetoelastic (ME) sensing system for the detection of classical swine fever virus (CSFV) is presented. The detection system comprises a test paper and a measurement circuit. The test paper consists mainly of an ME biosensor to detect the CSFV. Based on the impedance analysis technique, the measurement circuit is designed to measure the resonance frequency of the ME biosensor. The anti-CSFV IgG is immobilized onto the ME sensor surface to form the ME biosensor through a physical absorption approach. The experimental results show that the shift in the resonance frequency of the ME biosensor increases with the augmentation of the CSFV concentration. The effectiveness of the combination between the anti-CSFV IgG and CSFV is confirmed by the scanning electron microscopy (SEM) images, the sandwich-based enzyme-linked immunosorbent assay (ELISA) analysis, the interference study and the reference biosensor test method. The resonance frequency shift is linearly proportional to the concentration in the range from 0 to 2.5 μg/ml, and becomes sub-linear at higher concentrations. The ME biosensor for CSFV detection has a sensitivity of about 95 Hz/μg $\cdot$ ml^{-1}, with a detection limit of 0.6 μg/ml.

1. Introduction

Classical swine fever (CSF), caused by the classical swine fever virus (CSFV), is a devastating and highly contagious disease of swine which results in serious financial losses in the world (Edwards et al., 2000). Several countries, including Australia, Canada, New Zealand, the United States of America (USA) and some Member States of the European Union (EU), have successfully eradicated the virus through the implementation of strict control measures. However, in other parts of the world with significant pig production, the CSFV is still present, hindering the development of animal husbandry. Thus, it is included in the Office International des Epizooties (OIE) List A (Moennig, 2000).

During the past years, the CSFV detection has been extensively researched due to the substantial economic damage inflicted by this virus on the pig industry. Various methods have been developed for CSFV detection, such as RT-LAMP (Chen et al., 2010), flow cytometric analysis methods (Gunasekera et al., 2000), reverse transcriptase polymerase chain reaction (RT-PCR) analysis (Liu et al., 2011), colloidal gold-based immunochromatographic assay (Luo et al., 2014), and optical assay (Shen et al., 2007). However, these methods have some limitations, such as the long time required for sample preparation, complicated testing process, expensive instruments and costly maintenance.

Magnetoelastic (ME) sensors made of amorphous, ferromagnetic metallic glass ribbons, for example Metglas 2826MB, have received considerable attention because of their significant advantages of high sensitivity, low cost and wireless sensing. Due to the Joule effect, the ME sensor can vibrate longitudinally at a characteristic resonant frequency under the superimposition of both alternating (AC) and static (DC) magnetic fields (Quandt and Ludwig, 2000). The AC magnetic field is used to impart energy into the ME sensor, causing it to oscillate. The purpose of the DC magnetic field is to select the “operating point” on the magnetization curve of the sensor. As the resonant frequency is easily affected by the surrounding medium, the ME sensor can be used to measure different physical parameters including strain (Tan et al., 2008)/stress (Pereles et al., 2014), liquid density and viscosity (Jain et al., 2001), fluid flow velocity (Pereles et al., 2009) and the elastic modulus of thin films (Liang et al., 2007). Additionally, the resonant frequency of the ME sensor is sensitive to the mass change. The ME sensors modified with a chemical or biological sensing membrane can be used to detect a variety of bacteria, such as *Escherichia coli* (Ruan et al., 2003), *Bacillus anthracis* spores (Xie et al., 2014), *Salmonella typhimurium* (Park et al., 2013) and *Staphylococcal enterotoxin* B (Ruan et al., 2004).

* Corresponding author.
E-mail address: sangshengbo@tyut.edu.cn (S. Sang).

http://dx.doi.org/10.1016/j.bios.2016.03.067
0956-5663/

In this study, we have developed a detection system consisting of a test paper and a measurement circuit for the detection of CSFV. The measurement circuit is designed based on the impedance analysis technique. The test paper is fabricated by immobilizing an ME biosensor in a rectangular insulation supporting frame. The antibody against the CSFV is coated onto the ME biosensor surface through physical absorption. To evaluate the performance, test papers were immersed in the CSFV suspensions at different concentrations. The scanning electron microscopy (SEM), sandwich-based ELISA and the reference biosensor approach were separately used to confirm that the response signal is from the antibody-antigen binding of CSFV on the biosensor surface.

2. Theory and principle

Under the superimposition of both alternating and static magnetic fields, the ME sensor vibrates longitudinally. When the sensor vibrates at its resonance frequency, the conversion of the magnetic energy into elastic energy reaches a maximum. The resonance frequency (f_0) of the sensor with length L, density ρ, elastic module E, and Poisson's ratio v is given by Eq. (1) (Baimpos et al., 2012).

$$f_0=\frac{1}{2L}\sqrt{\frac{E}{\rho\left(1-v^2\right)}} \tag{1}$$

The resonance frequency of the ME sensor is sensitive to the mass change. For a small extra mass load of Δm on the sensor of mass M ($\Delta m \ll M$), the change in the resonance frequency (Δf) is given by Eq. (2) (Hiremath et al., 2015; Schmidt and Grimes, 2001).

$$\frac{\Delta f}{\Delta m}=-\frac{f_0}{2M} \tag{2}$$

From Eq. (2), it is clear that an extra mass load on the sensor surface results in a decrease in f_0. The anti-CSFV IgG is immobilized on the surface of the ME sensor to selectively adsorb the CSFV. Due to the combination of the antibody and antigen, the extra mass load on the biosensor increases, which in turn induces a decrease in the resonance frequency. In this way, the CSFV can be detected by monitoring the resonance frequency of the biosensor.

3. Detection system design

3.1. Measurement circuit design

Over the past years, three detecting methods have been developed to monitor the resonance frequency of the ME sensor, namely the time-domain measurement technique (Zeng et al., 2002), the frequency-domain measurement technique (Zeng et al., 2005) and the impedance de-tuning technique (Grimes et al., 1999). In the time-domain measurement technique, the ME sensor is excited by a sinusoidal magnetic field generated by a passing current through a coil. The sensor is interrogated by a pulse-like excitation signal, and the resonance frequency of the sensor is subsequently calculated by counting the number of oscillations per sensor ring-down time or using a Fast Fourier transform (FFT). The mechanism of the frequency-domain measurement technique consists in generating a sweep steady-state signal, and the response of the ME sensor is measured at every frequency point. The sensor resonance frequency is determined as the frequency at which the maximum response, such as the greatest output amplitude, is obtained. Due to its attributes of easy implementation and simple operation process, the impedance de-tuning technique is adopted in our design.

3.1.1. Impedance de-tuning technique principle

An ME sensor is inserted inside a solenoid coil, and an AC excitation signal is applied to the coil. A time varying magnetic field is generated inside the coil which drives the sensor to oscillate, with the vibration amplitude and phase being functions of the excitation frequency and impedance. Since the permeability of the sensor increases significantly at resonance, a sharp peak occurs at the resonance frequency of the solenoid's impedance spectrum. Thus, the resonance frequency of the sensor can be obtained by measuring the frequency at the sharp peak, as shown in Fig. S1.

3.1.2. Measurement circuit

The circuit based on the impedance analysis technique to characterize ME sensors was developed in a previous study (Zeng et al., 2006). For such a circuit, we made some improvements to certain elements, such as the new microcontroller that has a 12-bit multi-channel analog to digital converter on the chip, LCD display and USB communication interface. The block diagram of the circuit design in this study is shown in Fig. S1. The key components of the detector include the following:

Microcontroller: A STM32F103VET6 microcontroller (the ARM microcontroller family from STMicroelectronics Corporation) is chosen for its efficient bit manipulation and large embedded memory (512 KB of flash memory, 64 KB of SRAM). It has three 12-bit analog to digital converters on the chip and can work at frequencies up to 72 MHz. In this circuit, an 8 MHz crystal clock is used.

Direct digital synthesis (DDS): The DDS chip, AD9851, is used to digitally synthesize a sine wave of numerically controlled frequency from a reference clock. It is serially interfaced with the microcontroller. The crystal clock used in the DDS circuit is 30 MHz and provides a synthesized wave with a frequency resolution of 2 Hz.

RMS-to-DC converter: An RMS-to-DC converter, AD536A, is used to compute the true root-mean-square (RMS) value of the AC signal. It is a complete monolithic integrated circuit which performs a true RMS-to-DC conversion. The AD536A has a 450 kHz bandwidth and performs the RMS-to-DC conversion with the aid of an external capacitor.

DC biasing: A magnet is used to provide a DC biasing magnetic field that turns the sensor to an optimal operational point, facilitating sensor excitation and detection.

USB communication interface: The USB interface is adopted to communicate with the computer. The test data stored in the detector can be copied to the computer through such interface.

LCD display: An LCD is chosen to immediately display the impedance spectrum curve and the test resonance frequency value.

3.2. Test paper design

3.2.1. Preparation of the ME sensor platform

The ME strip-shaped sensor platform composed of the Metglas alloy 2826 ($Fe_{40}Ni_{40}P_{14}B_6$) was purchased from Honeywell Corporation (Morristown, NJ, USA), and cut into 5 mm × 1 mm × 0.028 mm using a computer-controlled laser cutting machine. The sensor platform was ultrasonically cleaned in ethanol for 15 min and rinsed with deionized water, to remove any debris and organic film on the sensor surface, and then dried in a stream of nitrogen. To protect the sensor platform from corrosion and to promote the immobilization of the antibody, both sides of the cleaned sensor platform were sputtered with chromium (100 nm thick), followed by gold (100 nm thick). The middle chromium layer enhances the adhesion between the gold and the sensor platform. The gold-coated sensor platform were annealed in a vacuum oven at 220 °C for 2 h to eliminate any residual stress in the sensor and improve adhesion of the gold layer to the ME

substrate. The annealed gold-coated sensor platform was ready (Fig. S2a) for antibody immobilization to form the biosensor and its resonance frequency in air is approximately 450 kHz.

3.2.2. Antibody immobilization

The gold-coated sensor platform was immersed in a 10 mM ethanol solution of 6-mercaptoundecanoic acid (purchased from Sigma-Aldrich Corporation, St. Louis, MO, USA) for 24 h at room temperature to form a self-assembled monolayer (SAM). The modified sensor platform was then removed from the solution and rinsed several times with ethanol to remove the unbonded thiols. The thiol-modified sensor platform was dipped into a solution containing 40 mM 1-ethyl-3-(3-dimethylaminopropyl) carbodiimide hydrochloride (EDC) and 10 mM N-hydroxysulfosuccinimide (NHS) in distilled water for 1 h to convert the terminal carboxylic groups to an active NHS ester, as shown in Fig. S2b. The sensor platform was subsequently rinsed with deionized water and dried under a stream of nitrogen. The anti-CSFV IgG (Green biological technology corporation, Ltd., China) was diluted in phosphate buffered saline (PBS buffer, 0.01 M, pH=7.4, Sigma-Aldrich) to prepare a 40 μg/ml antibody solution. The antibody was dispensed onto both sides of the sensor platform surface by immersing the sensor platform into a 1 ml antibody solution at 37 °C for 1 h. The excess antibody was removed by rinsing with PBS buffer solution, as shown in Fig. S2c. Then, the antibody-modified sensor platform was treated with 0.1% BSA for 30 min, to block the unreacted and non-specific sites. After rinsing with PBS buffer and deionized water, the sensor platform was dried under nitrogen. Then the ME biosensor is formed, as shown in Fig. S2d.

3.2.3. The test paper

The test paper consists of an ME biosensor and an insulation supporting frame with a rectangular groove, as shown in Fig. S3. The ME biosensor was fabricated by modifying the antibody on both sides of the ME sensor platform, as shown in Fig. S2. The biosensor was then fixed in the groove by linkers.

3.3. Signal measurement

In the experimental assay, the test papers were placed into the test tube containing 0.5 ml of the CSFV suspensions. The CSFV suspensions ranging from 0 to 10 μg/ml were prepared by serially diluting the concentrated virus suspension (1 mg/ml) with PBS buffer. All the test virus suspensions were stored at −20 °C in a refrigerator and moved to room temperature before use.

The test papers were subsequently exposed to the test virus suspensions at the concentrations of 0–10 μg/ml. The microcontroller-based measurement circuit was used to measure the resonance frequency of the biosensors at a resolution of 2 Hz. At each concentration, the resonance frequency of the biosensor was monitored and recorded for 45 min at an interval of 5 min. After the measurement, the biosensors were rinsed three times with deionized water and then the test papers were air-dried for SEM analysis.

3.4. Observation of CSFV on the ME biosensor surface

The CSFV captured on the surface of the biosensors were observed by SEM. Prior to SEM analysis, the biosensors were exposed to osmium tetroxide for 1 h at room temperature. The SEM observation was performed with a SU3500 SEM (Hitachi corporation, Tokyo, Japan) operated at 15 keV.

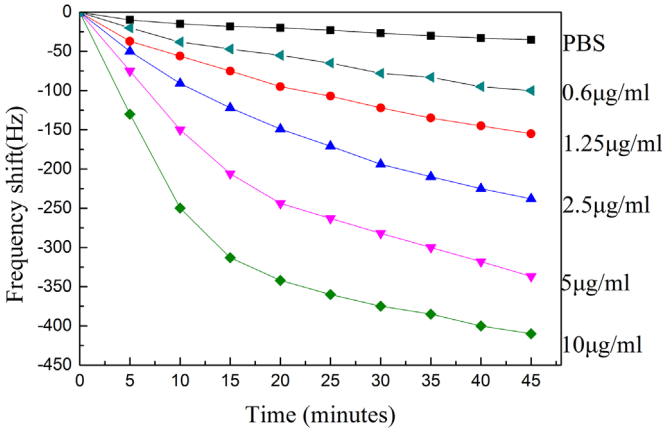

Fig. 1. Real-time response of the biosensor for different CSFV concentrations ranging from 0 to 10 μg/ml.

4. Results and discussion

4.1. Application of ME biosensor for CSFV detection

The dynamic response of the ME biosensor to the immune reaction on the biosensor surface is shown in Fig. 1, with CSFV concentration ranging from 0 to 10 μg/ml, as a function of the biosensor immersion time. When the biosensor was immersed in the CSFV suspension (pH=7.4) at 37 °C, the immune reaction between the immobilized antibody and the CSFV antigen led to the binding of CSFV molecule to the biosensor surface. Then, the anti-CSFV IgG proportionately combined to the CSFV antigen. Finally, the antibody-antigen complex formation led to a considerable increase in mass on the surface, which in turn caused a decrease in the biosensor's resonance frequency after an induction period, as illustrated in Fig. 1. The induction period is attributed to the time required for the combination. In general, the steady-state response is achieved in 45 minutes and, as can be seen in Fig. 1, the shift rate of the resonance frequency increases with the increase of the CSFV concentration. Additionally, a higher concentration of CSFV in the suspension can induce a larger shift in the resonance frequency. The results also indicate that there is a mass increase on the biosensor surface due to the combination between the anti-CSFV IgG and CSFV. The anti-CSFV IgG is a complex biomolecule made up of amino acids in an orderly arrangement. The organisms develop the antibody, a kind of protein, which can bind to a foreign molecule, such as the CSFV antigen. CSFV is an RNA virus, whose genome is characterized by positive polarity and polyprotein (Risatti et al., 2003). The capture of the CSFV antigen by the antibody is due to the protein affinity between the CSFV antigen and the anti-CSFV IgG. The interaction is more analogous to a lock and key arrangement (Nitilaksha and Hiremath, 2013). A schematic diagram of the interaction between the antibody and CSFV is depicted in Fig. S2e.

To verify that the response of the biosensor is only due to the CSFV, a contrast experiment was conducted without CSFV (PBS curve) which shows a noise level of ~35 Hz due to nonspecific binding. However, there is a 100-Hz change in resonance frequency at the 0.6 μg/ml CSFV concentration over the same time period, as shown in Fig. 1. Thus, there is only a small frequency change under this condition without specific binding between the anti-CSFV IgG and CSFV.

The shift in the resonance frequency versus CSFV concentration at the 45 min time point is plotted in Fig. 2. The shift in the resonance frequency is linearly proportional to the concentration in the range from 0 to 2.5 μg/ml. However, with the increase in concentration it becomes sub-linear, which indicates that the

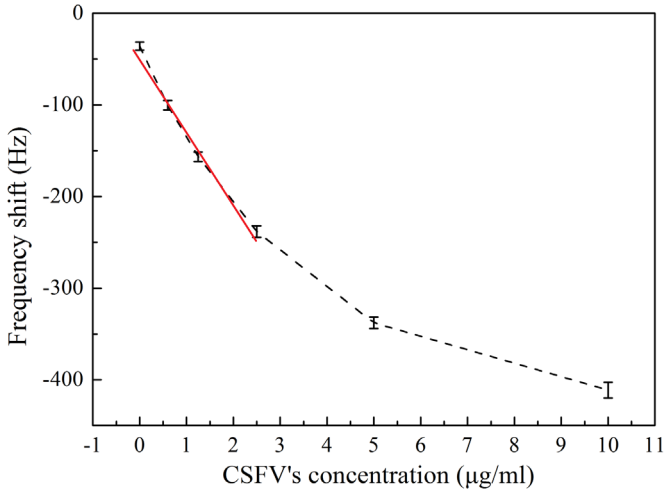

Fig. 2. The 45 min shift in the resonance frequency versus the CSFV concentration ranging from 0 to 10 μg/ml.

linearity is better at low CSFV concentrations. In the linear region, the detection sensitivity calculated from the resonance frequency shift is about 95 Hz/μg $\cdot$ ml^{-1}. In view of the high sensitivity, the method is suitable for the detection of CSFV.

4.2. Confirmation of anti-CSFV IgG and CSFV attachment on the biosensor

To confirm that the experimentally observed shifts in the resonance frequency is due to the attachment of CSFV to the biosensor surface, SEM was used to observe the biosensor surface before and after CSFV capture, as shown in Fig. 3. In this study, the antibody was covalently immobilized through the method of amine coupling to the gold surface modified with a self-assembled monolayer. The amine coupling introduces NHS esters into the surface of the self-assembled monolayer with the EDC-NHS solution. EDC as a coupling agent is used to activate carboxyl groups and a stable active ester is provided by the NHS. Then, the antibody is covalently linked to the activated NHS esters through the amide bond (Pei et al., 2001). With the anti-CSFV IgG immobilized on the sensor surface, there are a lot of ribbons in the shape of leaf, as shown in Fig. 3a. Each antibody consists of four polypeptides, specifically two heavy chains and two light chains joined to form a "Y" shaped molecule, just as illustrated in the principle diagram in Fig. S2c. Different antibodies have different amino acid sequences at the tips of the "Y", which are called antigen binding sites. These variable binding sites are composed of 110–130 amino acids and give the antibody its specificity and affinity for the binding antigen (Lange et al., 2008; Fu, 2010). When the antibody coated biosensors were exposed to the 10 μg/ml CSFV suspension, CSFV antigen molecules in the shape of a block were observed to be attached to the biosensor surface (Fig. 3b) through the cross-link between the antigen and the antibody (Krithiga et al., 2016). The binding force came from these non-covalent bonds between anti-CSFV IgG and CSFV, such as hydrogen bonds, hydrophobic force, salt bridges and Van der Waals forces (Mustafa et al., 2014; Honari et al., 2013). The clear antigen-antibody combining sites can be observed in Fig. 3c, there are cross-linking structures on the biosensor resulting from the combination between the anti-CSFV IgG and CSFV. The experiment illustrates that the CSFV antigen exhibits good binding capability with the anti-CSFV IgG.

In addition, the combination of anti-CSFV IgG and CSFV was assessed using a sandwich-based ELISA method. ELISA is commonly used for the detection of numerous viral proteins (Tong et al., 2016). The intensity of the yellow color was found to be proportional to the amount of immunocomplexes contained in each biosensor (Teijido et al., 2016). In this study, different biosensors bound to the CSFV at concentration ranging from 0 to 10 μg/ml were immersed into a 1 ml solution of 40 μg/ml horseradish peroxidase (HRP) conjugated anti-CSFV IgG solution for 1 h at 37 °C. The biosensors were then rinsed thoroughly with distilled water and PBS buffer. Subsequently, the biosensors were immersed in 1 ml of TMB substrate solution at room temperature in the dark for 10 min. The developing reaction was finally terminated by adding 1 ml 2 N H_2SO_4. Absorbance was read at 450 nm within 30 min after the developing reaction was halted. The experimental results indicate that the ELISA signals (OD 450 nm) rise as the CSFV concentration increases, as shown in Fig. 4, which further demonstrates that CSFV is successfully captured by the anti-CSFV IgG modified on the biosensor. The linear range is between 0 and 2.5 μg/ml.

To further demonstrate that the frequency shift is solely due to antibody-captured CSFV, a reference biosensor without antibody immobilization was employed. In addition, an interference study was carried out by testing the response of the ME biosensor to other antigens like porcine circovirus type2 (PCV2) and porcine pseudorabies virus (PRV). The shift in the resonance frequency of the reference biosensor exposed to 10 μg/ml of the CSFV suspension for 45 min was measured. During the test period, the shift in the resonance frequency of the detecting biosensor (Fig. 5, line d) increases faster than that of the reference biosensor (Fig. 5, line a). There is almost no change in the resonance frequency of the reference biosensor compared with the detecting biosensor under the same condition, namely, there is no CSFV absorbed due to the specific binding of the reference biosensor. The real-time response of the ME biosensors respectively immersed in 10 μg/ml of PCV2 solution and 10 μg/ml of PRV solution were observed. Actually, the biosensors showed little response to the interference of antigens like PCV2 (Fig. 5, line b) or PRV (Fig. 5, line c) due to nonspecific absorption. Together, all the observed results clearly indicate that

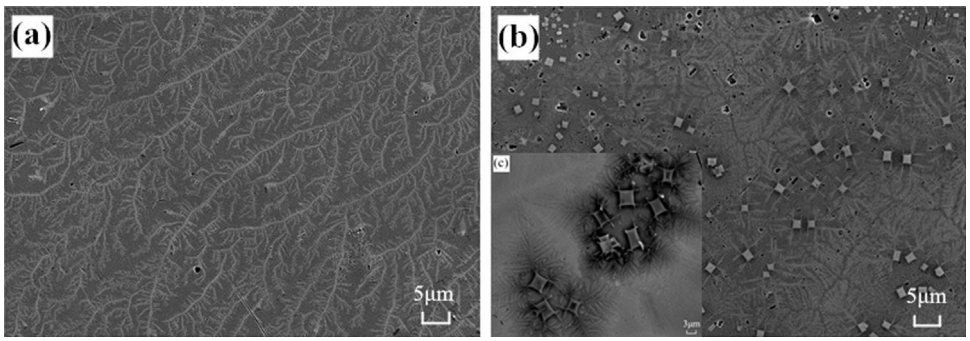

Fig. 3. SEM images of the biosensor surface before and after the capture of CSFV (a) biosensor surface before CSFV capture; (b) biosensor surface after CSFV capture.

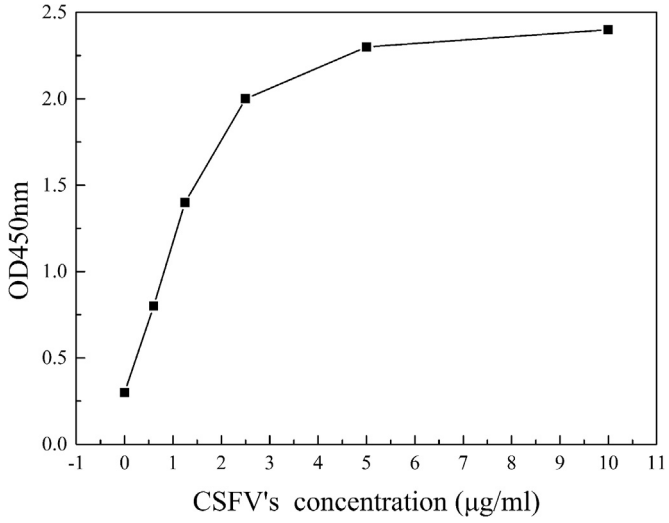

Fig. 4. Sandwich ELISA analysis performed on samples containing increasing concentrations of CSFV (0–10 μg/ml).

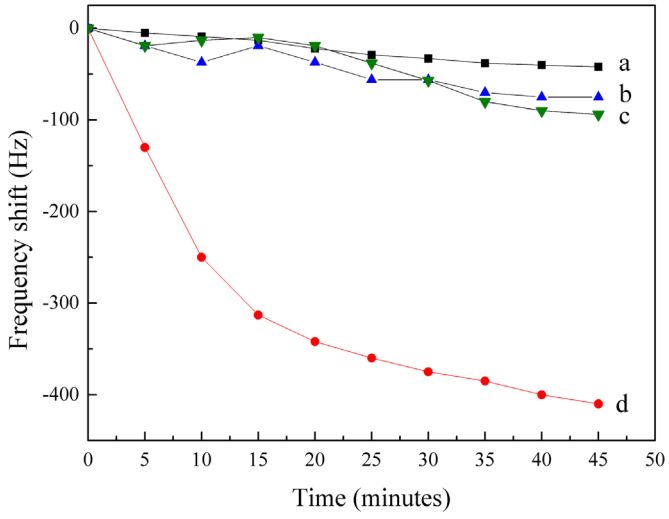

Fig. 5. Shift in the resonance frequency versus time when the detecting biosensor (Line d) and reference biosensor (Line a) are exposed to 10 μg/ml CSFV suspension under identical condition. Line b and line c show the responses of the ME biosensors exposed to 10 μg/ml of PCV2 solution and 10 μg/ml of PRV solution, respectively.

the resonance frequency shift is only due to the combination of the CSFV and the antibody modified on the ME biosensor surface.

5. Conclusions

In this study, an ME biosensor-based detection system for the detection of CSFV is presented. The detection system includes a measurement circuit and a test paper. Compared with the early electronic designs, our system has some advantages, such as simple circuit design, fast signal processing and visual LCD display. Due to the mass loading change induced by the combination of the CSFV and the anti-CSFV IgG on the biosensor surface, the resonance frequency of the ME biosensor varies. The shift in ME biosensor resonance frequency increases with the rise of the CSFV concentration, which is linearly proportional to the CSFV concentration ranging from 0 to 2.5 μg/ml and becomes sub-linear at higher concentrations. The sensitivity of the ME biosensor is approximately 95 Hz/μg · ml^{-1}. The detection limit of the ME biosensor in this study is about 0.6 μg/ml. Furthermore, the SEM observation, sandwich-based ELISA method and the reference biosensor approach prove that the shift in the resonance frequency is due to the antibody-antigen binding of CSFV on the biosensor surface. Future work will be focused on the improvement of the sensitivity for CSFV detection by decreasing the size of the ME biosensor.

Acknowledgements

This work is financially supported by the National Natural Science Foundation of China (Nos. 61471255, 61474079, 61501316, 51505324), Doctoral Fund of MOE of China (No. 20131402110013), 863 Project (2013AA041109, 2015AA042601).

Appendix A. Supporting information

Supplementary data associated with this article can be found in the online version at http://dx.doi.org/10.1016/j.bios.2016.03.067.

References

Baimpos, T., Gora, L., Nikolakis, V., Kouzoudis, D., 2012. Sens. Actuators A 186, 21–31.
Chen, L., Fan, X.Z., W., Wang, Q., Xu, L., Zhao, Q.Z., Zhou, Y.C., Liu, J., Tang, B., Zou, X. Q., 2010. Virol. Sin. 25, 59–64.
Edwards, S., Fukusho, A., Lefèvre, P.C., Lipowski, A., Pejsak, Z., Roehe, P., Westergaard, J., 2000. Vet. Microbiol. 73, 103–119.
Fu, L.L., 2010. Auburn University (Ph.D. thesis).
Gunasekera, T.S., Attfield, P.V., Veal, D.A., 2000. Appl. Environ. Microbiol. 66, 1228–1232.
Grimes, C.A., Ong, K.G., Loiselle, K., Stoyanov, P.G., Kouzoudis, D., Liu, Y., Tong, C., Tefiku, F., 1999. Smart Mater. Struct. 8, 639–646.
Hiremath, N., Guntupalli, R., Vodyanoy, V., Chin, B.A., Park, M.K., 2015. Sens. Actuators B 210, 129–136.
Honari, P., Allaudin, Z.N., Lila, M.A.M., Mustafa, N.H.B., 2013. Afr. J. Biotechnol. 10, 15795–15800.
Jain, M.K., Schmidt, S., Grimes, C.A., 2001. Appl. Acoust. 62, 1001–1011.
Krithiga, N., Viswanath, K.B., Vasantha, V.S., Jayachitra, A., 2016. Biosens. Bioelectron. 79, 121–129.
Luo, D.D., Xie, J., Li, X.Y., et al., 2014. Sichuan Anim. Vet. Sci. 41 (2), 39–41.
Liu, S.S., Zhao, Y., Hu, Q., Lv, C.C., Zhang, C.F., Zhao, R., Hu, F., Lin, W.C., Cui, S.J., 2011. J. Virol. Methods 172, 88–92.
Lange, K., Rapp, B.E., Rapp, M., 2008. Anal. Bioanal. Chem. 391, 1509–1519.
Liang, C., Prorok, B.C., 2007. J. Micromech. Microeng. 17, 709–716.
Mustafa, N., Allaudin, Z., Honari, P., Toung, O., Lila, M., 2014. Virol. Mycol. 3 2161–0517.1000.
Moennig, V., 2000. Vet. Microbiol. 73 (2–3), 93–102.
Nitilaksha P., Hiremath, 2013. Auburn University (Master thesis).
Pereles, B.D., DeRouin, A.J., Ong, K.G., 2014. J. Biomech. Eng. 136, 011010.
Park, M.K., Park, J.W., Wikle, H.C., Chin, B.A., 2013. Sens. Actuators B 176, 1134–1140.
Pereles, B.D., Shao, R., Tan, E.L., Ong, K.G., 2009. Smart Mater. Struct. 18, 095002.
Pei, R.J., Cheng, Z.L., Wang, E.K., Yang, X.R., 2001. Biosens. Bioelectron. 16, 355–361.
Quandt, E., Ludwig, A., 2000. Sens. Actuators A 81, 275–280.
Ruan, C.M., Zeng, K.F., Varghese, O.K., Grimes, C.A., 2004. Biosens. Bioelectron. 2, 138–144.
Ruan, C., Zeng, K.F., Varghesel, O.K., Grimes, C.A., 2003. Anal. Chem. 75, 6494–6498.
Risatti, G., Callahan, J., Nelson, W., Borca, M., 2003. J. Clin. Microbiol. 41, 500–505.
Shen, Z.H., Huang, M.C., Xiao, C., Zhang, Y., Zeng, X.Q., Wang, P.G., 2007. Anal. Chem. 79, 2312–2319.
Schmidt, S., Grimes, C.A., 2001. Sens. Actuators A 94, 189–196.
Tong, Q.H., Tao, T., Xie, L.Q., Lu, H.J., 2016. Biosens. Bioelectron. 80, 385–391.
Teijido, O., Ganesan, Y.T., Llanos, R., Peton, A., Urtecho, J.B., Soprani, A., Villamayor, A., Antonsson, B., Manon, S., Dejean, L., 2016. Anal. Biochem. 497, 90–94.
Tan, E.L., Pereles, B.D., Shao, R., Ong, J., Ong, K.G., 2008. Smart Mater. Struct. 17, 025015.
Xie, H., Chai, Y., Horikawa, S., Li, S., Chin, B.A., Wikle, H.C., 2014. Sens. Actuators A 205, 143–149.
Zeng, K.F., Ong, K.G., Yang, X.P., Grimes, C.A., 2006. Sens. Lett. 4, 388–397.
Zeng, K.F., Paulose, M., Ong, K.G., Grimes, C.A., 2005. Sens. Actuators A 121, 66–71.
Zeng, K.F., Ong, K.G., Mungle, C.S., Grimes, C.A., 2002. Rev. Sci. Instrum. 73, 4375–4380.